Photochemical & Photobiological Sciences

BODIPY-Embedded Electrospun Materials in Antimicrobial Photodynamic Inactivation

Photochemical & Photobiological Sciences

ARTICLE

BODIPY-Embedded Electrospun Materials in Antimicrobial Photodynamic Inactivation

Kevin R. Stoll [a,d], Frank Scholle [b], Jiadeng Zhu [c], Xiangwu Zhang [c] and Reza A. Ghiladi *[d]

Drug-resistant pathogens, particularly those that result in hospital acquired infections (HAIs), have emerged as a critical priority for the World Health Organization. To address the need for self-disinfecting materials to counter the threat posed by the transmission of these pathogens from surfaces to new hosts, here we investigated if a cationic BODIPY photosensitizer, embedded via electrospinning into nylon and polyacrylonitrile (PAN) nanofibers, was capable of inactivating both bacteria and viruses via antimicrobial photodynamic inactivation (aPDI). Materials characterization, including fiber morphology and the degree of photosensitizer loading, was determined by scanning electron microscopy (SEM), thermal gravimetric analysis (TGA), and UV-visible diffuse reflectance spectroscopy (UV-Vis DRS), and demonstrated that the materials were comprised of nanofibers (125-215 nm avg. diameter) that were thermostable to >300 °C. The antimicrobial potencies of the resultant **Nylon-BODIPY(+)** and **PAN-BODIPY(+)** nanofiber materials were evaluated against four strains of bacteria recognized by the World Health Organization as either critical or high priority pathogens: Gram-positive strains methicillin-resistant *S. aureus* (MRSA; ATCC BAA-44) and vancomycin-resistant *E. faecium* (VRE; ATCC BAA-2320), and Gram-negative strains multidrug-resistant *A. baumannii* (MDRAB; ATCC BAA-1605) and NDM-1 positive *K. pneumoniae* (KP; ATCC BAA-2146). Our results demonstrated the detection limit (99.9999%; 6 log units reduction in CFU/mL) photodynamic inactivation of three strains upon illumination (30-60 min; 40-65±5 mW/cm^2; 400-700 nm): MRSA, VRE, and MDRAB, but only minimal inactivation (47-75%) of KP. Antiviral studies employing **PAN-BODIPY(+)** against vesicular stomatitis virus (VSV), a model enveloped virus, revealed complete inactivation. Taken together, the results demonstrate the potential for electrospun **BODIPY(+)**-embedded nanofiber materials as the basis for pathogen-specific anti-infective materials, even at low photosensitizer loadings.

1 Introduction

In 2017, the World Health Organization (WHO) released a "global priority list of antibiotic-resistant bacteria to guide research, discovery, and the development of new antibiotics" to combat the threat posed by these pathogens.[1] The 12 families of bacteria that pose the greatest threat to human health were grouped into three priority levels: 'Critical', 'High', and 'Medium'. Critical pathogens, including *Acinetobacter baumannii* (AB) and Enterobacteriaceae such as *Klebsiella pneumoniae* (KP), are multidrug-resistant bacteria that pose a particular threat in healthcare settings (i.e., contribute to the proliferation of hospital acquired infections, or HAIs) as they have become resistant to most antibiotics, including last-line

defences. Similarly, 'High' priority pathogens, e.g., vancomycin-resistant *Enterococcus faecium* (VRE) and methicillin-resistant *Staphylococcus aureus* (MRSA), also contribute to HAIs, and are becoming increasingly resistant to antibiotic treatment. While antibiotics will remain on the front lines of the fight against infectious diseases, the ability of various bacterial strains to develop resistance to these drugs remains an issue, and drives the need for alternative or complementary methods for controlling pathogen transmission.

One such method that provides an opportunity to inactivate various microbes *prior* to human infection is antimicrobial photodynamic inactivation (aPDI).[2] In aPDI, illumination of a photosensitizer (PS) by visible or near infrared light in the presence of molecular oxygen generates singlet oxygen ($^1O_2$, Type II mechanism) and other reactive oxygen species (ROS, Type I mechanism);[3] these biocides react in a non-targeted approach against a variety of microbes (including both Gram-positive and -negative bacteria, viruses with capsid or lipid envelopes, fungi/yeasts, and mycobacteria), leading to their inactivation.[4-9] Given the indiscriminate mode of action of these ROS, resistance to singlet oxygen is believed to be unlikely.[10-13] Moreover, as aPDI operates in a manner independent from traditional antibiotics, aPDI has been shown to be equally effective against pathogens that are resistant to conventional

[a.] Department of Chemistry, United States Air Force Academy, CO 80840, USA.
[b.] Department of Biological Sciences, North Carolina State University, Raleigh, NC 27695-7614, USA.
[c.] Fiber and Polymer Science Program, Department of Textile Engineering, Chemistry and Science, North Carolina State University, Raleigh, NC 27695-8301, USA.
[d.] Department of Chemistry, North Carolina State University, Raleigh, NC 27695-8204, USA.
*Correspondence: reza_ghiladi@ncsu.edu; Tel.: +1-919-389-1716; Fax: +1-919-515-5079.
† Electronic Supplementary Information (ESI) available: Modified Synthesis of **BODIPY(+)**. See DOI: 10.1039/x0xx00000x

antibiotics when compared with their drug-susceptible counterparts.[2, 14]

While momentum continues to increase for photodynamic therapy as a treatment for infectious diseases *in vivo*, there is an emerging window of opportunity for developing self-sterilizing materials using photodynamic inactivation to prevent pathogen transmission *ex vivo*.[15] To this end, several classes of materials based upon a photodynamic mode of action have been reported: in terms of scaffolds, natural polymer materials have spanned cellulose nanocrystals,[16-20] cellulose acetate,[21] cellulose fibers,[22-24] and cotton fabrics[25-27], while synthetic polymer materials have included polyacrylonitrile, polyurethane, olefinic block copolymers, polystyrene, polyvinyl alcohol, polycaprolactone, nylon, and polyamide-6,[28-36] to name a few. These natural and artificial polymer-based photodynamic materials incorporated several different classes of photosensitizers, including porphyrins [e.g., free-base or zinc tetraphenylporphyrin, cationic 5,10,15,20-tetrakis(1-methylpyridinium-4-yl)porphyrin (TMPyP), PPIX], phthalocyanines, phenothiazine dyes such as methylene blue and toluidine blue O, and xanthine dyes such as rose bengal and phloxine B. Antimicrobial activity was demonstrated against bacteria (e.g., Gram-positive *Staphylococcus aureus*, vancomycin-resistant *Enterococcus faecium*, and Gram-negative *Escherichia coli*, *Acinetobacter baumannii*, *Pseudomonas aeruginosa*, and *Klebsiella pneumonia*), viruses (e.g., polyomavirus, dengue-1, baculovirus, influenza A, and human adenovirus-5) and fungi (*Aspergillus fumigatus*).

While these aforementioned systems have focused on more traditional photosensitizers (porphyrins, phenothiazines, and phthalocyanines), relatively few studies have investigated the applicability of boron dipyrromethene[37-39] (a.k.a. BODIPY)-based compounds as potential photosensitizers for infection control via materials-based aPDI. Stemming from the seminal work of Yogo,[40] O'Shea,[41] and Banfi,[42-44] BODIPY photosensitizers have been shown to be highly effective in mediating the photodynamic inactivation of pathogens in solution. Specific to this report, we have shown that 2,6-diiodo-1,3,5,7-tetramethyl-8-(N-methyl-4-pyridel)-4,4'-difluoroboradiazaindacene (DIMPy-BODIPY), henceforth referred to here as **BODIPY**[(+)], exhibits antiviral, antibacterial and antifungal photodynamic inactivation at nanomolar concentrations and short illumination times.[6] However, questions exist regarding the scope and applicability of BODIPY-based PS, and more specifically **BODIPY**[(+)], for mediating aPDI in materials. For example, can a cationic BODIPY PS be successfully incorporated via non-covalent methods into a material without significant leaching? Does the **BODIPY**[(+)] PS exhibit both antibacterial and antiviral activities when incorporated into a material? How does the presence of a single cationic group in **BODIPY**[(+)] alter the PS loading, and ultimately the efficacy of the resultant material, when compared to more highly charged porphyrin-based PS?

To address these questions, here we have investigated if cationic **BODIPY**[(+)]-embedded electrospun nylon and polyacrylonitrile (PAN) nanofibers, namely **Nylon-BODIPY**[(+)] and **PAN-BODIPY**[(+)] (Figure 1), were capable of inactivating both

bacteria and viruses via antimicrobial photodynamic inactivation. The **BODIPY**[(+)] PS was selected owing to ability to effectively mediate antimicrobial photodynamic inactivation that was previously attributed to its cationic charge, a property that has been shown to favor aPDI via increased electrostatic interactions with the negatively charged cell wall components of both Gram-positive and Gram-negative bacteria.[43, 45, 46] We selected electrospinning given it is a relatively simple and inexpensive technique that creates consistent and uniform fiber materials from polymer powders.[47] Electrospun fibers possess a number of characteristics important for aPDI, including a high surface area that allows for increased PS/pathogen interaction. Electrospinning also allows for the embedment of photosensitizers without the need for their functionalization,[28, 29, 31-34, 36, 48-50] opening the door to a wide variety of commercially-available or easily-synthesized photosensitizers to be implemented regardless of size, functional groups, or charge. In addition, because the polymer and photosensitizer are combined in solution prior to electrospinning, there is minimal variation in the uniformity of the material, i.e. no "hot spots". As will be shown, the results obtained here demonstrate the potential for electrospun **BODIPY**[(+)]-embedded nanofiber materials as the basis for pathogen-specific anti-infective materials.
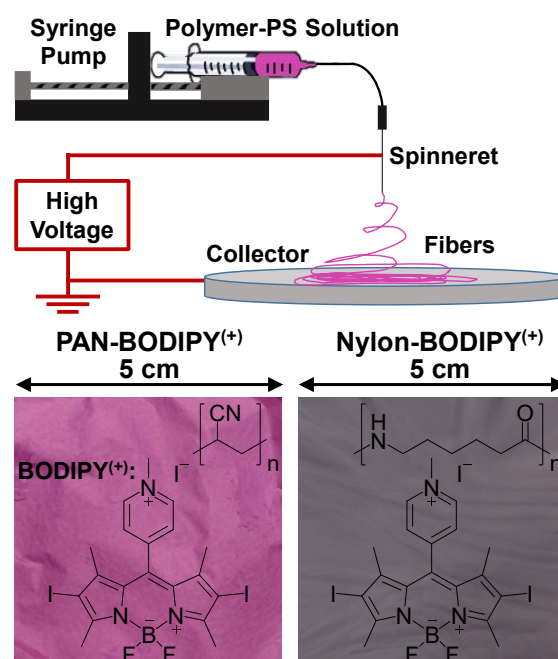

Figure 1. Electrospinning schematic (top), and photographic images of **PAN-BODIPY**[(+)] (bottom left, pink) and **Nylon-BODIPY**[(+)] (bottom right, grey).

2 Experimental Section

2.1 Materials

Buffer salts, Criterion agar (bacteriological grade) and ampicillin were from Fisher Scientific. Nutrient broths were purchased from commercial vendors (Tryptic Soy Broth, BD Difco Nutrient Broth #234000, and BD Difco Bacto Brain Heart Infusion

#237500 from BD Biosciences; LB-Media from Teknova). Tetracycline was purchased through Shelton Scientific. All other bioreagents and solvents were purchased from commercial sources and used as received unless otherwise noted. Ultrapure deionized water used for all media and buffers was provided by an Easypure II system (Barnstead). The cationic **BODIPY(+)** photosensitizer [2,6-diiodo-1,3,5,7-tetramethyl-8-(N-methyl-4-pyridyl)-4,4'-difluoroboradiazaindacene] was synthesized per literature protocol,[6, 42-44] with minor modifications as detailed in the Supporting Information.

2.2 Instrumentation

UV-visible absorption measurements were recorded using a Cary Bio50 UV-Vis Spectrophotometer (Agilent). Scanning electron microscopy data were gathered on a FEI Verios 460L field-emission scanning electron microscope (FESEM). Optical density measurements were gathered on a Thermo Electron Crop. Genesys 10 UV scanning spectrophotometer. Thermal gravimetric analysis data were collected on a SDT Q600 under argon/oxygen (80/20) at 10 °C/ min.

2.3 Electrospinning

For **Nylon-BODIPY(+)** nanofibers, Nylon-6 (5-50 micron particle size) was purchased from Sigma-Aldrich (St. Louis, MO, USA) and used as received. The solution was prepared by firstly dissolving the nylon powder into formic acid as a solvent at 12 wt % (nylon:formic acid), followed by the addition of the **BODIPY(+)** photosensitizer (at 10 wt.% with respect to the mass of nylon-6). The solution was further stirred for 24 h prior to electrospinning in an apparatus that employed a Gamma ES40P-20W/DAM variable high voltage (20 kV) power supply. The flow rate applied was 0.1 mL/h. The needle-to-collector distance was set at 15 cm, and electrospun fibers were collected on aluminium foil.

For **PAN-BODIPY(+)** nanofibers, polyacrylonitrile (PAN, M_w = 150,000) was purchased from Sigma-Aldrich (St. Louis, MO, USA) and used as received. The solution was prepared by first dissolving PAN powder into DMF solvent at 5 wt % (PAN : DMF), and allowed to stir for over 24 h, followed by the addition of the **BODIPY(+)** photosensitizer (at 10 wt.% with respect to the mass of PAN). The solution was further stirred for 24 h prior to electrospinning as described above for **Nylon-BODIPY(+)**, with the following parameters: the collector plate distance remained at 15 cm, however the voltage was decreased to 15 kV and the feed rate was increased to 0.75 mL/h.

Upon completion of the electrospinning process, the materials were stored at room temperature in a dark environment to prevent photobleaching. **PAN-BODIPY(+)** samples were lightly shaken in one mL phosphate-buffered saline (PBS) at room temperature for one minute. The samples were washed in this manner seven times. **Nylon-BODIPY(+)** samples were washed together at room temperature for 16 hours in 50 mL PBS at 100 RPM. Materials were considered fully washed when the concentration of **BODIPY(+)** removed during the washing was less than 10 nM as verified by UV-visible spectroscopy (data not shown), which is below the level

required to observe solution-based inactivation of bacteria with this PS.[6]

2.4 Antimicrobial Photodynamic Inactivation Studies

2.4.1 PDI Instrumentation. All bacteria were cultured at 37 °C in either a VWR Incubating Mini Shaker (400 rpm) or a New Brunswick Scientific Excella E24 Incubator Shaker (250 rpm). A Thermo Electron Corporation Genesys 10 UV-Vis scanning spectrophotometer was used for the measurement of optical densities. Bacterial pelleting was conducted in a Thermo Electron Corporation Sorvall® Legend RT centrifuge. A LumaCare USA model LC122 PDT non-coherent light source was employed for all antimicrobial photodynamic inactivation studies. The lamp was equipped with an OSRAM 64653 HLX Xenophot bulb (250 W, 24 V), and employed a LUM V (400–700 nm band pass filter) fiber optic probe with a ~95 ± 3% average transmittance (T_{avg}). Fluence rates were measured in units of mW/cm^2 with an Ophir Orion power meter.

2.4.2 Bacterial Culture Conditions. Bacterial strains were grown to an initial concentration of 1-4×10^8 CFU/mL as determined by optical density measurements at 600 nm (OD$_{600}$) using previously established growth curves. Multi-drug resistant *Acinetobacter baumannii* (AB; ATCC BAA-1605) was grown in LB-Miller broth with 5 μg/mL tetracycline; methicillin-resistant *Staphylococcus aureus* (MRSA; ATCC BAA-44) was grown in tryptic soy broth (TSB) with 5 μg/mL tetracycline; *Klebsiella pneumoniae* (KP; ATCC BAA-2146) was grown in BD Difco Nutrient Broth #234000 with 100 μg/mL ampicillin; vancomycin-resistant *Enterococcus faecium* (VRE; ATCC BAA-2320) was grown in BD Difco Bacto Brain Heart Infusion #237500 with 100 mg/L ampicillin. Cultures were then pelleted via centrifugation at 3700 g for 10 min, the supernatant was decanted, and the bacteria were resuspended in 5 mL of phosphate buffer saline (PBS; aqueous solution of 170 mM NaCl, 3.4 mM KCl, 10.0 mM Na$_2$HPO$_4$, 1.8 mM KH$_2$PO$_4$, pH 7.2) containing 0.05% Tween-80.

2.4.3 Bacterial Inactivation Studies

Inactivation studies were performed using two sterile, flat-bottom 24-well plates (BD Falcon): one for the illuminated samples and the second for the dark control. Four material samples were cut to precisely fit the well bottom (~1 cm diam.) using a custom hole punch, three for the illuminated plate and one in the dark control plate. Aliquots (400 μL) of cell culture were transferred to each well, and incubated in the dark as follows: MRSA - no dark incubation period; VRE, KP, and MDRAB - 60 min dark incubation period. After the dark incubation period, the light study plate was subjected to visible (400–700 nm) light illumination: MRSA was illuminated for 30 minutes at 40±5 mW/cm^2, while VRE, KP, and MDRAB were illuminated for 60 minutes at 65±5 mW/cm^2. The dark control plate remained in the dark for the duration of the illumination period.

Upon completion of the illumination period, 10 μL of the bacterial solution from the illuminated plate was serially diluted at 1:10 in PBS five times. The six samples (5 dilutions and 1

undiluted sample) were plated and incubated at 37 °C overnight. The dark control was serially diluted in the same manner twice in duplicate, resulting in 4 dark control plates that were also incubated at 37 °C overnight. Finally, the original bacterial solution in PBS was serially diluted and plated as described above as a compound free control. Following the incubation period, the colony forming units (CFU) were counted and the illuminated samples were compared to the dark controls (assigned 100% survival) to determine the percent survivability of the bacteria. Statistical significance was assessed using an unpaired Student's two-tailed t-test.

2.4.4 Viral Inactivation Studies. Vero E6 cells were employed to propagate (and titer by plaque assay) vesicular stomatitis virus (VSV) NJ strain. 25 μL of the viral stock (~1×10⁶ plaque forming units (PFU)/mL) were added either empty well (control), and **Nylon-BODIPY⁽⁺⁾** / **PAN-BODIPY⁽⁺⁾** containing wells of a 96-well plate in the dark. The plates were subjected to visible (400–700 nm; 65±5 mW/cm²; 60 min) light illumination as described above for the antibacterial assay, or were kept in the dark for the control experiments. Studies were performed in biological triplicates. After illumination, 100 μL of minimum essential medium (MEM) supplemented with 1% FBS, 10 mM HEPES and antibiotics were added to wash remaining viruses off the materials. Viruses were subsequently titered by serial dilution (10-fold) using Vero cells in 24-well plates at 37 °C. VSV concentration was determined by plaque assay using crystal violet staining to visualize the plaques 24 h after infection.

3 Results and Discussion

3.1 Materials Characterization

3.1.1 Electrospinning and Photosensitizer Loading

BODIPY⁽⁺⁾-embedded nanofibers were prepared by a simple mixing of the pre-dissolved polymer (nylon-6 or PAN) with the **BODIPY⁽⁺⁾** photosensitizer, followed by electrospinning. Formic acid and DMF were used as solvents for nylon-6 and PAN, respectively. The weights of **BODIPY⁽⁺⁾** photosensitizer and PAN in this study were 0.1 g and 1 g, while the weights of **BODIPY⁽⁺⁾** photosensitizer and nylon-6 were 0.24 g and 2.4 g. Application of the requisite high voltage and collection on an aluminum foil target yielded the **Nylon-BODIPY⁽⁺⁾** (grey) and **PAN-BODIPY⁽⁺⁾** (pink) nanofiber materials shown in Figure 1. Interestingly, despite containing the identical photosensitizer, their visual appearance differed, likely attributable to a combination of differences in PS-loading and/or PS/polymer local environment (*vide infra*). Prior to any characterization or antimicrobial studies, the **BODIPY⁽⁺⁾**-embedded nanofibers were thoroughly washed to remove adventitiously bound **BODIPY⁽⁺⁾** photosensitizer.[48]

To determine the degree of photosensitizer loading, the washed materials were dried in an incubator overnight (37 °C), weighed, and subsequently dissolved in 1 mL of the solvent used in the electrospinning process (formic acid for nylon-6; DMF for PAN). Once the material was fully dissolved, 9 mL of acetone (nylon) or water (PAN) was added, the sample was centrifuged, and the UV-vis spectrum of the supernatant was acquired. Utilizing the published molar absorptivity coefficients for **BODIPY⁽⁺⁾** in water[6] and acetone[43] (75,900 M⁻¹cm⁻¹ and 110,000 M⁻¹cm⁻¹, respectively), the amount of **BODIPY⁽⁺⁾** per milligram of material was calculated using the Beer-Lambert law. The PS-loading in **Nylon-BODIPY⁽⁺⁾** was found to be 3.4 nmol/mg material (0.25 wt%), while for **PAN-BODIPY⁽⁺⁾** the PS-loading was 21.1 nmol/mg material (1.51 wt%). This six-fold difference in PS-loading is a major contributing factor to the difference in appearance between the two materials (Figure 1), and likely reflects the degree of non-covalent interaction between the nylon-6 or polyacrylonitrile scaffolds and the **BODIPY⁽⁺⁾** PS. These PS-loadings are lower than that of our previously studied PS-embedded electrospun material, PAN-Por⁽⁺⁾ (34.8 nmol/mg material)[48] that was produced in an identical manner, and suggests that the Por⁽⁺⁾ photosensitizer was better retained in the polymer matrix than **BODIPY⁽⁺⁾**, possibly due to: i) charge - the polar nitrile group of PAN possess a high dipole moment (3.9 D[51]) that likely forms a stronger electrostatic interaction with the tetracationic Por⁽⁺⁾ over the monocationic **BODIPY⁽⁺⁾**; and ii) size – the larger Por⁽⁺⁾ is likely better encapsulated than the smaller **BODIPY⁽⁺⁾** PS. When compared with covalent PS-polymer scaffolds, the degree of PS loading in **BODIPY⁽⁺⁾**-embedded nanofibers is on a par with previously studied PS-cellulose conjugates Por⁽⁺⁾-paper (12.4 nmol PS/mg)[22] and BC-10-PPIX (13.0 nmol PS/mg)[24], but significantly less than Por⁽⁺⁾-CNCs (cellulose nanocrystals, 160 nmol PS/mg)[17] and RC-TETA-PPIX-Zn nanofibers (412 nmol PS/mg material).[23] The effect of PS loading on antimicrobial activity, particularly with respect to the inactivation of Gram-negative bacteria, will be discussed later (*vide infra*).

3.1.2 Scanning electron microscopy

Scanning electron microscopy (SEM) was used to confirm the nanofiber nature of the electrospun materials (Figure 2). When compared to pure electrospun nylon-6 (Figure 2B; 123 nm avg. diameter), **Nylon-BODIPY⁽⁺⁾** (Figure 2A; 215 nm avg. diameter) exhibited a 1.75x larger fiber diameter, but the fiber morphology was otherwise unaffected by the photosensitizer, with both materials exhibiting smooth fiber surfaces (see insets). **PAN-BODIPY⁽⁺⁾** (Figure 2C; 125 nm avg. diameter) and pure PS-free electrospun polyacrylonitrile (Figure 2D; 126 nm avg. diameter) were virtually identical in size, and both exhibited a somewhat rougher fiber surface than the corresponding nylon materials. By way of comparison, the previously studied material PAN-Por⁽⁺⁾ exhibited a ~175 nm avg. diameter,[48] with a similarly rough surface morphology as to that of **PAN-BODIPY⁽⁺⁾**. While the photosensitizer charge (monocationic **BODIPY⁽⁺⁾** vs. tetracationic Por⁽⁺⁾), polymer dielectric (nylon-6 vs. PAN), and polymer solvent (formic acid/nylon-6 vs. DMF/PAN) likely play roles in modulating the fiber diameter in electrospinning, overall the results obtained here demonstrated the nanofiber nature of the **BODIPY⁽⁺⁾**-embedded electrospun materials.
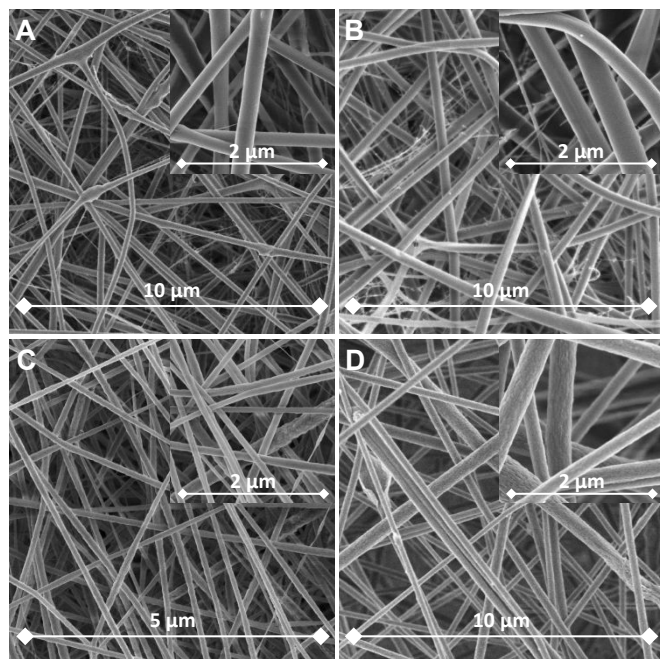
Figure 2. SEM images for (A) **Nylon-BODIPY**[(+)], (B) pure electrospun nylon-6, (C) **PAN-BODIPY**[(+)], and (D) pure electrospun PAN. Materials were coated in gold/palladium to increase image quality at higher magnification.

3.1.3 UV-vis Diffuse Reflectance Spectroscopy

UV-vis diffuse reflectance spectra were obtained for both **Nylon-BODIPY**[(+)] and **PAN-BODIPY**[(+)] and compared to the solution spectrum of **BODIPY**[(+)] in acetone (Figure 3). Both materials exhibited an absorption maximum at 553 nm, a ~7 nm bathochromic shift from that of **BODIPY**[(+)] in acetone (546 nm). Such bathochromic shifts have been previously attributed to the differences in the local environment (e.g., polarity, solvation) of the photosensitizer when covalently appended or embedded within a polymer matrix vs. the solution spectrum.[17, 22-24] Despite exhibiting the same absorption maxima, **Nylon-BODIPY**[(+)] ($A_{580}/A_{553} = 0.75$) had a slightly more intense absorption shoulder at 580 nm than **PAN-BODIPY**[(+)] ($A_{580}/A_{553} = 0.67$), but similar A_{408}/A_{553} ratios (0.28 vs 0.29, respectively). We suggest that the six-fold lower photosensitizer loading and lower intensity absorption at 580 nm for **PAN-BODIPY**[(+)] when compared with **Nylon-BODIPY**[(+)] are together responsible for the visual color differences between the two materials as seen in Figure 1.
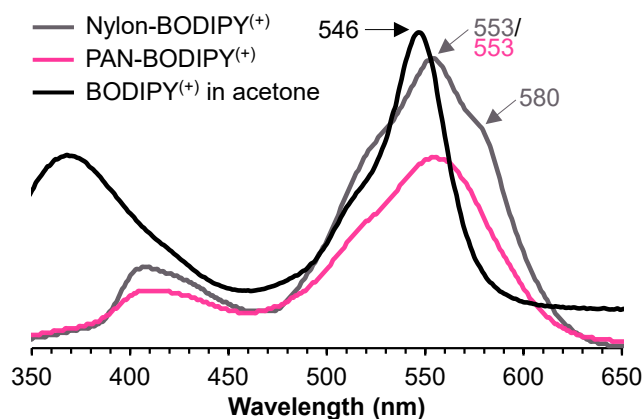

Figure 3. UV-vis diffuse reflectance spectra of **Nylon-BODIPY**[(+)] (grey) and **PAN-BODIPY**[(+)] (pink) in comparison to the solution spectrum of **BODIPY**[(+)] in acetone (black).

3.1.4 Thermal gravimetric analysis

The thermal decomposition profiles of **Nylon-BODIPY**[(+)] and **PAN-BODIPY**[(+)] were investigated using thermal gravimetric analysis (Figure 4). In the first stage up to 100 °C, a minor initial weight loss of ~2-3% was noted for both materials, and was attributed to the loss of absorbed water. For **Nylon-BODIPY**[(+)], a minimal 5% total weight loss was noted up to 300 °C, with a minor stage of decomposition (to 10% total weight loss) with an onset temperature at 330 °C, and a main stage of decomposition with an onset temperature of 360 °C. For **PAN-BODIPY**[(+)], a minor ~3% weight loss was noted with an onset temperature of 150 °C, and likely corresponds to the loss of residual DMF solvent from the electrospinning process. A more significant main stage of decomposition (to ~25% total weight loss) was noted with an onset temperature of 300 °C, with a second, more gradual decomposition noted after 325 °C. When compared to pure nylon-6 (424 °C)[52] and PAN (302 °C),[53] the presence of the **BODIPY**[(+)] does not appear to affect the thermal decomposition behaviour of the resultant materials, consistent with the low PS loadings of < 1.5 wt%.
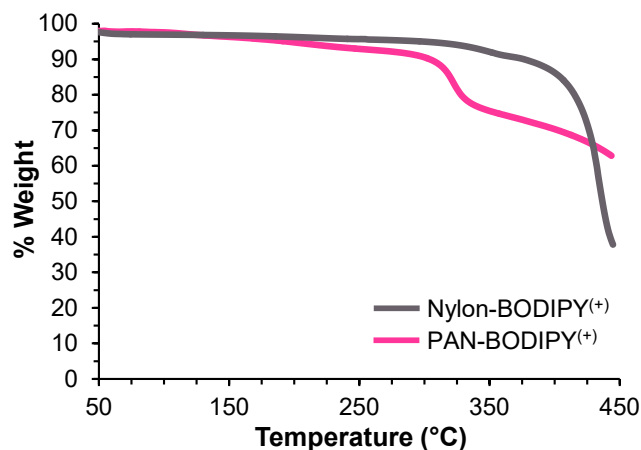

Figure 4. Thermal gravimetric analysis of electrospun **Nylon-BODIPY**[(+)] (grey) and **PAN-BODIPY**[(+)] (pink).

3.2 Antimicrobial Photodynamic Inactivation

3.2.1 Antibacterial Activity

In vitro aPDI assays employing **Nylon-BODIPY⁽⁺⁾** and **PAN-BODIPY⁽⁺⁾** were performed using non-coherent visible light (400–700 nm) for 30 min (40±5 mW/cm²) against MRSA, or 60 min (65±5 mW/cm²) against VRE, MDRAB, and KP. Additionally, a 60 minute dark incubation period was employed for these latter three bacteria prior to illumination, as dark incubation has been shown to improve the interaction of nanoscale materials with bacteria that originally start in a solution phase.[16, 17]

Against two Gram-positive bacteria (Figure 5), methicillin-resistant *S. aureus* ATCC BAA-44 (MRSA) and vancomycin-resistant *E. faecium* ATCC BAA-2320 (VRE), both **Nylon-BODIPY⁽⁺⁾** (Figure 5A) and **PAN-BODIPY⁽⁺⁾** (Figure 5B) achieved detection limit inactivation (99.9999%, 6 log units reduction in CFU/mL; MRSA: P = 0.0016; VRE: P = 0.0045). In other words, no colony forming units (CFU) were observed after illumination. By contrast, no statistically significant inactivation was observed for either material in the absence of light when compared with the material free controls, demonstrating the requirement for light (as expected) for antibacterial photodynamic inactivation. While these results are comparable to those achieved with the previously studied electrospun material PAN-Por⁽⁺⁾ (i.e., detection-level inactivation of *S. aureus* and VRE),[48] we note here the 10-fold lower PS loading of **Nylon-BODIPY⁽⁺⁾** (3.4 nmol/mg material vs 35 nmol/mg material for PAN-Por⁽⁺⁾), as well as a lower fluence rate (40 mW/cm² vs. 65 mW/cm² employed for PAN-Por⁽⁺⁾). Similarly, the PS-cellulose conjugates Por⁽⁺⁾-paper (12.4 nmol PS/mg)[22] and Por⁽⁺⁾-CNCs (160 nmol PS/mg)[17] achieved 4-6 log units of inactivation of *S. aureus*/MRSA and VRE, yet required higher PS-loading or a significantly more tedious covalent attachment route than the simple PS-embedding strategy employed here for **Nylon-BODIPY⁽⁺⁾** and **PAN-BODIPY⁽⁺⁾**.
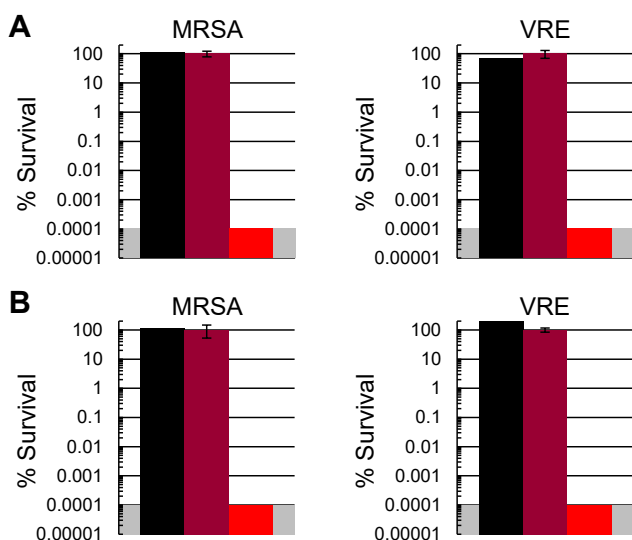

Figure 5. Photodynamic inactivation studies employing electrospun materials (A) **Nylon-BODIPY⁽⁺⁾** and (B) **PAN-BODIPY⁽⁺⁾** against Gram-positive bacteria methicillin-resistant *S. aureus* ATCC BAA-44 (MRSA), and vancomycin-resistant *Enterococcus faecium* ATCC BAA-2320 (VRE). For both panels, displayed are the material-free (cells-only) dark control (black bars), PS-embedded material dark controls set to 100% (dark red), and the illuminated studies (red) displayed as the percent survival of the material dark control. See text for illumination conditions. As the plating technique employed to determine % survival did not allow for detection of survival rates of <0.0001%, data points below the detection limit were set to 0.0001% survival for graphing purposes and are indicated by the grey shaded area.

When surveyed against two drug-resistant Gram-negative bacteria, multi-drug resistant *A. baumannii* strain ATCC BAA-1605 (MDRAB) and NDM-1 positive *K. pneumoniae* strain ATCC BAA-2146 (KP), a much wider range of susceptibilities to **Nylon-BODIPY⁽⁺⁾** (Figure 6A) and **PAN-BODIPY⁽⁺⁾** (Figure 6B) was observed. MDRAB was found to be highly susceptible to photodynamic inactivation, exhibiting 99.95% (3.7 log units; P = 0.0014) reduction in viable cells with **Nylon-BODIPY⁽⁺⁾**, and detection limit inactivation (99.9999%; 6 log units; P = 0.004) with **PAN-BODIPY⁽⁺⁾**, consistent with the 6-fold higher PS-loading of the latter material (*vide supra*). *K. pneumoniae*, however, proved to be highly tolerant to photodynamic inactivation by these materials, with a reduction in viable cells by a modest 47% (~0.7 log units; P = 0.0014) for **Nylon-BODIPY⁽⁺⁾**, and 75% (~0.9 log units; P = 0.03) inactivation by **PAN-BODIPY⁽⁺⁾**. While the results against MDRAB are comparable between **PAN-BODIPY⁽⁺⁾**, PAN-Por⁽⁺⁾,[48] and the PS-cellulose conjugates Por⁽⁺⁾-Paper[22] and Por⁽⁺⁾-CNCs,[16] the poor level of photodynamic inactivation of KP was unexpected, as our previous studies employing photosensitizers in solution (TMPyP, methylene blue, and DIMPy-BODIPY)[6] or embedded/covalently attached to materials (Por⁽⁺⁾-Paper,[22] PAN-Por⁽⁺⁾,[48] ZnTMPyP⁴⁺/OBC26[35]) have consistently demonstrated that KP is susceptible to photodynamic inactivation, albeit it less so than the other strains studied here. We surmise that the lower PS-loadings of **Nylon-BODIPY⁽⁺⁾** and **PAN-BODIPY⁽⁺⁾** are the likely explanation as to their lower efficacy against KP. However, another key factor may be the presence of three cationic charges for Por⁽⁺⁾ versus the single cationic charge of **BODIPY⁽⁺⁾**: cationic charges on the PS have been shown to be beneficial for the inactivation of Gram-negative bacteria via increased electrostatic PS/bacteria association owing to the negative surface charge of the bacteria.[2] As with the Gram-positive strains, the dark controls showed no statistically significant inactivation, again demonstrating the requirement of light for the photodynamic inactivation of MDRAB and KP.
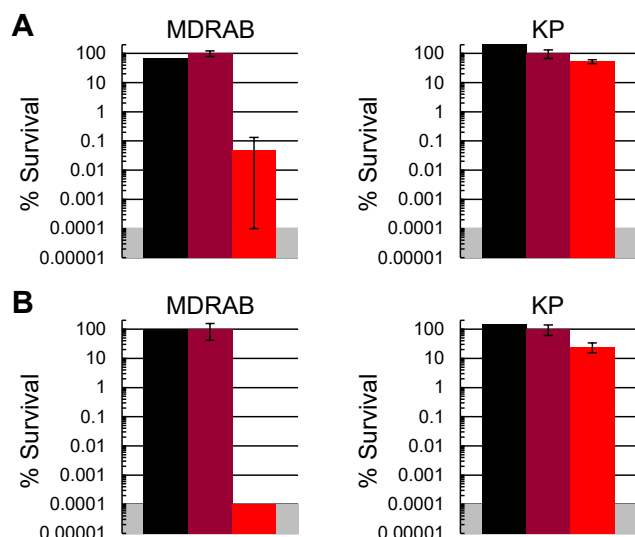
Figure 6. Photodynamic inactivation studies employing electrospun materials (A) **Nylon-BODIPY(+)** and (B) **PAN-BODIPY(+)** against Gram-negative bacteria multidrug-resistant *A. baumannii* ATCC BAA-1605 (MDRAB), and NDM-1 positive *K. pneumoniae* ATCC BAA-2146 (KP), For both panels, displayed are the material-free (cells-only) dark control (black bars), PS-embedded material dark controls set to 100% (dark red), and the illuminated studies (red) displayed as the percent survival of the material dark control. See text for illumination conditions. Detection limits were as described in Figure 5.

3.2.2 Antiviral Activity

Antiviral photodynamic inactivation studies employing **PAN-BODIPY(+)** were conducted against the model enveloped vesicular stomatitis virus (VSV) (Figure 7), using illumination conditions similar to those of the antibacterial studies (65 ± 5 mW/cm^2, 400-700 nm, 1 h). Impressively, detection limit inactivation (67 PFU/mL) of VSV was observed (99.99%, 4 log units; $P = 0.0058$). We have previously noted detection level inactivation of VSV with PAN-Por(+)[48] and ZnTMPyP^{4+}/OBC26[35], but demonstrate here a similar efficacy despite the lower PS-loading of **PAN-BODIPY(+)**. VSV inactivation of ~1 log unit was also noted in the **PAN-BODIPY(+)** dark control. Given the strong antiviral activity shown by the material when illuminated, we suggest that the dark inactivation resulted from the minimal light exposure needed to perform the biological assays. We note that previous photodynamic materials with strong antiviral character have also displayed 'dark' inactivation that was attributed to incidental light exposure.[6, 22, 35, 48]
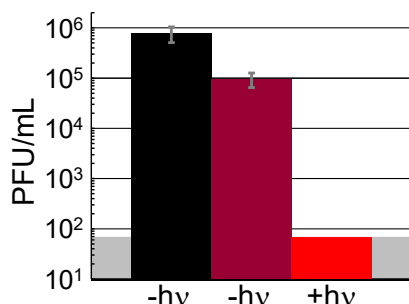

Figure 7. Antiviral photodynamic inactivation studies employing **PAN-BODIPY(+)** against vesicular stomatitis virus (VSV). Displayed are the material-free (cells-only) dark control (black), the **PAN-BODIPY(+)** dark control (dark red), and the illuminated study of **PAN-BODIPY(+)** (red). Illumination conditions were as follows: 400-700 nm, 65±5 mW/cm^2, 60

min. The minimal detection limit was 67 PFU/mL and is indicated by the shaded grey region.

3.2.3 Photobleaching Studies

Our previous work with the **BODIPY(+)** photosensitizer suggested that it undergoes photobleaching after 30 min illumination at 400–700 nm, 65 ± 5 mW/cm^2 (total fluence of 118 J/cm^2).[6] However, we have noted before that embedding a PS (or covalent conjugation) within a polymer provides additional protection against photobleaching, likely from reduced PS/PS interaction.[22, 48] Here, we investigated the ability for both **Nylon-BODIPY(+)** and **PAN-BODIPY(+)** to inactivate methicillin-resistant *S. aureus* ATCC BAA-44 (MRSA) after the materials had been illuminated for an extended time ('photo-aged') prior to the antibacterial light study being performed.

The studies were carried out as described in section 3.2.1, however, the washed materials were pre-illuminated with 11 hours (**Nylon-BODIPY(+)**) or 9 hours (**PAN-BODIPY(+)**) of light (400-700 nm, 65 ± 5 mW/cm^2) prior to performing the standard aPDI assay. As seen in Figure 8, the photobleached samples of both **Nylon-BODIPY(+)** (Figure 8A) and **PAN-BODIPY(+)** (Figure 8B) performed equally well as to the pristine (non-photobleached) materials (Figure 5), with detection level inactivation observed for both (6 log units; $P < 0.005$). These results demonstrate that the embedding of the photosensitizer in either nylon-6 or polyacrylonitrile are both capable of providing the **BODIPY(+)** photosensitizer with prolonged efficacy as a result of reduced PS photobleaching.
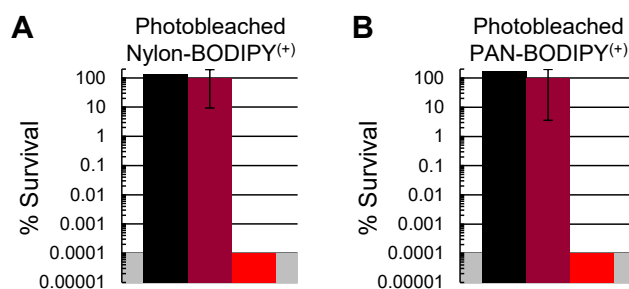

Figure 8. Photodynamic inactivation studies against methicillin-resistant *S. aureus* ATCC BAA-44 (MRSA) employing 'photo-aged' electrospun materials (A) **Nylon-BODIPY(+)** and (B) **PAN-BODIPY(+)**. The two materials were illuminated (400-700 nm, 65 ± 5 mW/cm^2) for 9 h (**Nylon-BODIPY(+)**) or 11 h (**PAN-BODIPY(+)**) prior to the aPDI assay being performed. For both panels, displayed are the material-free (cells-only) dark control (black bars), PS-embedded material dark controls set to 100% (dark red), and the illuminated studies (red) displayed as the percent survival of the material dark control. The antibacterial light study illumination conditions and detection limits were as described in Figure 5 for MRSA.

4 Conclusions

We have demonstrated the successful embedding of a cationic **BODIPY(+)** photosensitizer into nylon and polyacrylonitrile nanofibers via electrospinning. This method affords reasonable scalability without the need for custom-synthesized photosensitizers or polymers that detract from the widespread adoption of photodynamic materials. Although the electrospinning of the two materials was performed in nearly

identical fashion, the degree of photosensitizer loading varied 6-fold between the two, and shows how polymer-specific non-covalent interactions between the polymer scaffold and the PS can affect the retention of the embedded photosensitizer, and ultimately the photodynamic properties of the resultant materials: although photosensitizer loading did not factor into the detection limit inactivation of Gram-positive bacteria MRSA and VRE, differential activity was seen in the case of Gram-negative bacteria, and the higher PS-loaded material was needed to achieve detection limit inactivation of MDRAB. Against KP, however, neither **Nylon-BODIPY(+)** nor **PAN-BODIPY(+)** showed significant inactivation, and was likely due to either a lower PS-loading when compared to other PS-embedded materials, or the use of a monocationic **BODIPY(+)** photosensitizer here rather than the tri/tetracationic porphyrin-based photosensitizers used in those other materials. Our results here are consistent with previous observations that Gram-negative bacteria are typically more tolerant of photodynamic inactivation than Gram-positive species due to the highly impermeable lipopolysaccharides contained in their outer membrane, and suggest the use of higher PS-loading or increased cationic charge in the design of future photodynamic antimicrobial materials. Gratifyingly, however, was the detection limit inactivation of vesicular stomatitis virus that demonstrates the multifaceted capability of a single photodynamic material to inactivate multiple species of microbes (i.e., bacteria and viruses). Moreover, embedding of the **BODIPY(+)** photosensitizer into a polymer appears to extend its lifetime against photobleaching, showing that PS-selection based solely upon solution studies does not necessarily correlate to longevity of that PS for aPDI applications in materials. Taken together, the results obtained here show the promise of **BODIPY(+)** photosensitizers for use in electrospun aPDI materials as a viable, scalable, and potentially effective means to prevent the spread of hospital acquired infections and other harmful microbes through the use of self-sterilizing surfaces.

Conflicts of interest

There are no conflicts to declare.

Acknowledgements

References

1 World Health Organization, Global Priority List of Antibiotic-Resistant Bacteria to Guide Research, Discovery, and Development of New Antibiotics, *WHO Priority Pathogens List for R&D of New Antibiotics*, 2017.

2 M. R. Hamblin, Antimicrobial photodynamic inactivation: a bright new technique to kill resistant microbes, *Curr. Opin. Microbiol.*, 2016, **33**, 67-73.

3 L. Huang, Y. Xuan, Y. Koide, T. Zhiyentayev, M. Tanaka and M. R. Hamblin, Type I and Type II mechanisms of antimicrobial photodynamic therapy: An in vitro study on gram-negative and gram-positive bacteria, *Lasers Surg. Med.*, 2012, **44**, 490-499.

4 E. Feese and R. A. Ghiladi, Highly efficient in vitro photodynamic inactivation of *Mycobacterium smegmatis*, *J. Antimicrob. Chemother.*, 2009, **64**, 782-785.

5 T. Ito and K. Kobayashi, *In Vivo* Evidence for the Photodynamic Membrane Damage as a Determining Step of the Inactivation of Yeast Cells Sensitized by Toluidine Blue, *Photochem. Photobiol.*, 1977, **25**, 399-401.

6 B. L. Carpenter, X. Situ, F. Scholle, J. Bartelmess, W. W. Weare and R. A. Ghiladi, Antiviral, Antifungal and Antibacterial Activities of a BODIPY-Based Photosensitizer, *Molecules*, 2015, **20**, 10604-10621.

7 L. Sobotta, P. Skupin-Mrugalska, J. Mielcarek, T. Goslinski and J. Balzarini, Photosensitizers Mediated Photodynamic Inactivation Against Virus Particles, *Mini-Rev. Med. Chem.*, 2015, **15**, 503-521.

8 T. Dai, B. B. Fuchs, J. J. Coleman, R. A. Prates, C. Astrakas, T. G. St Denis, M. S. Ribeiro, E. Mylonakis, M. R. Hamblin and G. P. Tegos, Concepts and principles of photodynamic therapy as an alternative antifungal discovery platform, *Front. Microbiol.*, 2012, **3**, 120.

9 L. Costa, M. A. Faustino, M. G. Neves, A. Cunha and A. Almeida, Photodynamic inactivation of mammalian viruses and bacteriophages, *Viruses*, 2012, **4**, 1034-1074.

10 A. Tavares, C. M. Carvalho, M. A. Faustino, M. G. Neves, J. P. Tome, A. C. Tome, J. A. Cavaleiro, A. Cunha, N. C. Gomes, E. Alves and A. Almeida, Antimicrobial photodynamic therapy: study of bacterial recovery viability and potential development of resistance after treatment, *Mar. Drugs*, 2010, **8**, 91-105.

11 S. P. Tseng, L. J. Teng, C. T. Chen, T. H. Lo, W. C. Hung, H. J. Chen, P. R. Hsueh and J. C. Tsai, Toluidine blue O photodynamic inactivation on multidrug-resistant pseudomonas aeruginosa, *Lasers Surg. Med.*, 2009, **41**, 391-397.

12 D. M. Vera, M. H. Haynes, A. R. Ball, T. Dai, C. Astrakas, M. J. Kelso, M. R. Hamblin and G. P. Tegos, Strategies to potentiate antimicrobial photoinactivation by overcoming resistant phenotypes, *Photochem. Photobiol.*, 2012, **88**, 499-511.

13 F. Giuliani, M. Martinelli, A. Cocchi, D. Arbia, L. Fantetti and G. Roncucci, In vitro resistance selection studies of RLP068/Cl, a new Zn(II) phthalocyanine suitable for antimicrobial photodynamic therapy, *Antimicrob. Agents Chemother.*, 2010, **54**, 637-642.

14 T. Maisch, A new strategy to destroy antibiotic resistant microorganisms: antimicrobial photodynamic treatment, *Mini Rev. Med. Chem.*, 2009, **9**, 974-983.

15   S. Noimark, C. W. Dunnill and I. P. Parkin, Shining light on materials - a self-sterilising revolution, *Adv. Drug Del. Rev.*, 2013, **65**, 570-580.

16   B. L. Carpenter, E. Feese, H. Sadeghifar, D. S. Argyropoulos and R. A. Ghiladi, Porphyrin-cellulose nanocrystals: a photobactericidal material that exhibits broad spectrum antimicrobial activity, *Photochem. Photobiol.*, 2012, **88**, 527-536.

17   E. Feese, H. Sadeghifar, H. S. Gracz, D. S. Argyropoulos and R. A. Ghiladi, Photobactericidal porphyrin-cellulose nanocrystals: synthesis, characterization, and antimicrobial properties, *Biomacromolecules*, 2011, **12**, 3528-3539.

18   N. Drogat, R. Granet, V. Sol, C. Le Morvan, G. Begaud-Grimaud, F. Lallouet and P. Krausz, O108: Cellulose nanocrystals: A new chlorin carrier designed for photodynamic therapy: Synthesis, Characterization and Potent Anti-Tumoural Activity, *Photodiagn. Photodyn. Ther.*, 2011, **8**, 157-157.

19   F. Le Guern, T.-S. Ouk, K. Grenier, N. Joly, V. Lequart and V. Sol, Enhancement of photobactericidal activity of chlorin-e6-cellulose nanocrystals by covalent attachment of polymyxin B, *J. Mater. Chem. B*, 2017, **5**, 6953-6962.

20   N. Drogat, R. Granet, C. Le Morvan, G. Begaud-Grimaud, P. Krausz and V. Sol, Chlorin-PEI-labeled cellulose nanocrystals: synthesis, characterization and potential application in PDT, *Bioorg. Med. Chem. Lett.*, 2012, **22**, 3648-3652.

21   M. Krouit, R. Granet and P. Krausz, Photobactericidal plastic films based on cellulose esterified by chloroacetate and a cationic porphyrin, *Bioorg Med Chem*, 2008, **16**, 10091-10097.

22   B. L. Carpenter, F. Scholle, H. Sadeghifar, A. J. Francis, J. Boltersdorf, W. W. Weare, D. S. Argyropoulos, P. A. Maggard and R. A. Ghiladi, Synthesis, Characterization, and Antimicrobial Efficacy of Photomicrobicidal Cellulose Paper, *Biomacromolecules*, 2015, **16**, 2482-2492.

23   J. Dong, R. A. Ghiladi, Q. Wang, Y. Cai and Q. Wei, Protoporphyrin-IX conjugated cellulose nanofibers that exhibit high antibacterial photodynamic inactivation efficacy, *Nanotechnology*, 2018, **29**, 265601.

24   J. Dong, R. A. Ghiladi, Q. Wang, Y. Cai and Q. Wei, Protoporphyrin IX conjugated bacterial cellulose via diamide spacer arms with specific antibacterial photodynamic inactivation against *Escherichia coli*, *Cellulose*, 2018, **25**, 1673-1686.

25   C. Ringot, V. Sol, M. Barriere, N. Saad, P. Bressollier, R. Granet, P. Couleaud, C. Frochot and P. Krausz, Triazinyl Porphyrin-Based Photoactive Cotton Fabrics: Preparation, Characterization, and Antibacterial Activity, *Biomacromolecules*, 2011, **12**, 1716-1723.

26   C. Ringot, V. Sol, R. Granet and P. Krausz, Porphyrin-grafted cellulose fabric: New photobactericidal material obtained by "Click-Chemistry" reaction, *Mater. Lett.*, 2009, **63**, 1889-1891.

27   W. Chen, W. Wang, X. Ge, Q. Wei, R. A. Ghiladi and Q. Wang, Photooxidation Properties of Photosensitizer/Direct Dye Patterned Polyester/Cotton Fabrics, *Fiber Polym.*, 2018, **19**, 1687-1693.

28   Y. Lhotakova, L. Plistil, A. Moravkova, P. Kubat, K. Lang, J. Forstova and J. Mosinger, Virucidal nanofiber textiles based on photosensitized production of singlet oxygen, *PLoS One*, 2012, **7**, e49226.

29   S. Jesenska, L. Plistil, P. Kubat, K. Lang, L. Brozova, S. Popelka, L. Szatmary and J. Mosinger, Antibacterial nanofiber materials activated by light, *J. Biomed. Mater. Res. A*, 2011, **99**, 676-683.

30   J. Mosinger, O. Jirsak, P. Kubat, K. Lang and B. Mosinger, Bactericidal nanofabrics based on photoproduction of singlet oxygen, *J. Mater. Chem.*, 2007, **17**, 164-166.

31   J. Mosinger, K. Lang, P. Kubat, J. Sykora, M. Hof, L. Plistil and B. Mosinger, Jr., Photofunctional polyurethane nanofabrics doped by zinc tetraphenylporphyrin and zinc phthalocyanine photosensitizers, *J. Fluoresc.*, 2009, **19**, 705-713.

32   P. Henke, K. Lang, P. Kubat, J. Sykora, M. Slouf and J. Mosinger, Polystyrene nanofiber materials modified with an externally bound porphyrin photosensitizer, *ACS Appl. Mater. Interfaces*, 2013, **5**, 3776-3783.

33   J. Dolansky, P. Henke, P. Kubat, A. Fraix, S. Sortino and J. Mosinger, Polystyrene Nanofiber Materials for Visible-Light-Driven Dual Antibacterial Action via Simultaneous Photogeneration of NO and $O_2(^1\Delta_g)$, *ACS Appl. Mater. Interfaces*, 2015, **7**, 22980-22989.

34   M. Arenbergerova, P. Arenberger, M. Bednar, P. Kubat and J. Mosinger, Light-activated nanofibre textiles exert antibacterial effects in the setting of chronic wound healing, *Exp. Dermatol.*, 2012, **21**, 619-624.

35   B. S. T. Peddinti, F. Scholle, R. A. Ghiladi and R. J. Spontak, Photodynamic Polymers as Comprehensive Anti-Infective Materials: Staying Ahead of a Growing Global Threat, *ACS Appl. Mater. Interfaces*, 2018, **10**, 25955-25959.

36   J. R. Kim and S. Michielsen, Photodynamic antifungal activities of nanostructured fabrics grafted with rose bengal and phloxine B against Aspergillus fumigatus, *J. Appl. Polym. Sci.*, 2015, **132**, 42114.

37   R. Ziessel, G. Ulrich and A. Harriman, The chemistry of Bodipy: A new El Dorado for fluorescence tools, *New J. Chem.*, 2007, **31**, 496-501.

38   A. Loudet and K. Burgess, BODIPY dyes and their derivatives: syntheses and spectroscopic properties, *Chem. Rev.*, 2007, **107**, 4891-4932.

39   W. J. Peveler, S. Noimark, H. Al-Azawi, G. B. Hwang, C. R. Crick, E. Allan, J. B. Edel, A. P. Ivanov, A. J. MacRobert and I. P. Parkin, Covalently Attached Antimicrobial Surfaces Using BODIPY: Improving Efficiency and Effectiveness, *ACS Appl. Mater. Interfaces*, 2018, **10**, 98-104.

40   T. Yogo, Y. Urano, Y. Ishitsuka, F. Maniwa and T. Nagano, Highly Efficient and Photostable Photosensitizer Based on BODIPY Chromophore, *J. Am. Chem. Soc.*, 2005, **127**, 12162-12163.

41   D. O. Frimannsson, M. Grossi, J. Murtagh, F. Paradisi and D. F. O'Shea, Light induced antimicrobial properties of a brominated boron difluoride (BF_2) chelated tetraarylazadipyrromethene photosensitizer, *J. Med. Chem.*, 2010, **53**, 7337-7343.

42 S. Banfi, G. Nasini, S. Zaza and E. Caruso, Synthesis and photophysical properties of a series of BODIPY dyes, *Tetrahedron*, 2013, **69**, 4845-4856.

43 E. Caruso, S. Banfi, P. Barbieri, B. Leva and V. T. Orlandi, Synthesis and antibacterial activity of novel cationic BODIPY photosensitizers, *J. Photochem. Photobiol. B*, 2012, **114**, 44-51.

44 S. Banfi, E. Caruso, S. Zaza, M. Mancini, M. B. Gariboldi and E. Monti, Synthesis and photodynamic activity of a panel of BODIPY dyes, *J. Photochem. Photobiol. B*, 2012, **114**, 52-60.

45 E. Reddi, M. Ceccon, G. Valduga, G. Jori, J. C. Bommer, F. Elisei, L. Latterini and U. Mazzucato, Photophysical Properties and Antibacterial Activity of Meso-substituted Cationic Porphyrins, *Photochem. Photobiol.*, 2002, **75**, 462-470.

46 A. Minnock, D. I. Vernon, J. Schofield, J. Griffiths, J. H. Parish and S. B. Brown, Mechanism of Uptake of a Cationic Water-Soluble Pyridinium Zinc Phthalocyanine across the Outer Membrane of Escherichia coli, *Antimicrob. Agents Chemother.*, 2000, **44**, 522-527.

47 D. Li and Y. Xia, Electrospinning of Nanofibers: Reinventing the Wheel?, *Adv. Mater.*, 2004, **16**, 1151-1170.

48 S. Stanley, F. Scholle, J. Zhu, Y. Lu, X. Zhang, X. Situ and R. Ghiladi, Photosensitizer-Embedded Polyacrylonitrile Nanofibers as Antimicrobial Non-Woven Textile, *Nanomaterials*, 2016, **6**, 77.

49 P. Henke, H. Kozak, A. Artemenko, P. Kubát, J. Forstová and J. Mosinger, Superhydrophilic Polystyrene Nanofiber Materials Generating O2(1Δg): Postprocessing Surface Modifications toward Efficient Antibacterial Effect, *ACS Appl. Mater. Interfaces*, 2014, **6**, 13007-13014.

50 J. Mosinger, K. Lang, L. Plíštil, S. Jesenská, J. Hostomský, Z. Zelinger and P. Kubát, Fluorescent Polyurethane Nanofabrics: A Source of Singlet Oxygen and Oxygen Sensing, *Langmuir*, 2010, **26**, 10050-10056.

51 Q.-Y. Wu, X.-N. Chen, L.-S. Wan and Z.-K. Xu, Interactions between Polyacrylonitrile and Solvents: Density Functional Theory Study and Two-Dimensional Infrared Correlation Analysis, *The Journal of Physical Chemistry B*, 2012, **116**, 8321-8330.

52 C. Carrizales, S. Pelfrey, R. Rincon, T. M. Eubanks, A. Kuang, M. J. McClure, G. L. Bowlin and J. Macossay, Thermal and mechanical properties of electrospun PMMA, PVC, Nylon 6, and Nylon 6,6, *Polym. Adv. Technol.*, 2008, **19**, 124-130.

53 I. M. Alarifi, A. Alharbi, W. S. Khan, A. Swindle and R. Asmatulu, Thermal, Electrical and Surface Hydrophobic Properties of Electrospun Polyacrylonitrile Nanofibers for Structural Health Monitoring, *Materials (Basel)*, 2015, **8**, 7017-7031.

54

TOC Entry (19 words)
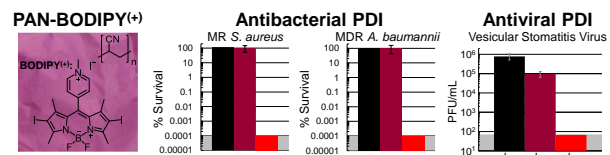
Electrospun BODIPY$^{(+)}$-embedded nanofiber materials were capable of the detection-level photodynamic inactivation of drug-resistant Gram-positive and Gram-negative bacteria and viruses.